Maejo Int. J. Sci. Technol. **2024**, *18*(01), 75-87

Maejo International Journal of Science and Technology

ISSN 1905-7873; e- ISSN: 2697-4746
Available online at www.mijst.mju.ac.th

Full Paper

Pneumonia detection by deep learning models based on image processing method: A novel approach

Ahmet Çelik [1, *] and Semih Demirel [2]

[1] Department of Computer Technologies, Tavsanlı Vocational School, Kutahya Dumlupinar University, 43300 Kütahya, Turkey
[2] Department of Computer Engineering, Faculty of Engineering, Kutahya Dumlupinar University, 43300 Kütahya, Turkey
* Corresponding author, e-mail: ahmet.celik@dpu.edu.tr

Received: 10 November 2023 / Accepted: 14 March 2024 / Published: 21 March 2024

Abstract: Pneumonia is a common and challenging disease to treat. Diagnosis of pneumonia is performed by analysing chest X-ray images with a specialist doctor today. This situation can create an excessive workload for doctors and prolong the diagnosis time. Performing early and accurate diagnosis of pneumonia using pre-trained deep learning models, which are a subcategory of the deep learning method, can be extremely beneficial. Using computer-aided diagnosis systems increases the accuracy of pneumonia diagnosis and thanks to these systems, doctors have an idea about the disease before diagnosis. In this study chest X-Ray images were classified as healthy or pneumonia using pre-trained deep learning methods. The histogram equalisation image processing method was used to improve image quality and the mask region-based convolutional neural network pre-trained method was used to segment the chest region. Alexnet, ResNet18 and VGG16 pre-trained models were used for image classification as healthy and pneumonia. ResNet18 showed outstanding performance in this study. According to the performance metrics of accuracy (0.983), recall (0.994) and F1-score (0.987), success rates were achieved by using the ResNet18 model. This study has shown that deep learning models can achieve high success rates in pneumonia diagnosis.

Keywords: pneumonia detection, chest X-Ray image, histogram equalisation, mask R-CNN, image segmentation, deep learning

INTRODUCTION

Lung diseases are quite common worldwide due to factors such as climate change, environmental pollution, tobacco smoking, allergens, viruses, bacteria, or fungi. Commonly encountered lung diseases include pneumonia, tuberculosis, fibrosis, obstructive and asthma.

Maejo Int. J. Sci. Technol. **2024**, *18*(01), 75-87

Pneumonia is a condition that occurs with the blockage of air sacs in the lungs [1]. It is a serious lung infection that, if not diagnosed and treated promptly, can be life-threatening. Therefore, early detection of pneumonia is crucial for successful treatment. Computer-aided diagnostic systems can assist in diagnosing the disease by processing examination findings, benefiting both patients and doctors. This capability facilitates correct disease diagnosis in the early period within a short time.

The primary cause of pneumonia, a lung condition, is an infection resulting from bacteria, viruses and fungi. Early diagnosis of the disease is crucial for the success of the treatment process. Currently, chest diseases are diagnosed through the examination of chest X-ray images by a radiologist. However, relying solely on the visual observation of pneumonia in chest X-ray images can complicate the diagnostic process and may lead to misdiagnosis due to other hidden diseases.

Early diagnosis of pneumonia and prompt treatment can halt the progression of the disease to a fatal stage [2]. Accurate diagnosis of pneumonia from X-ray images forms the foundation for timely treatment [3]. Radiologists or doctors visually examine chest X-rays to identify critical signs and lesions. Developing a machine learning model to address such situations would be highly beneficial for both doctors and patients. During periods of high patient influx, such as epidemics, the workload on doctors and hospital systems increases significantly. Intelligent diagnostic tools can prove useful in efficiently diagnosing diseases during unexpected situations, as exemplified during the 2019 Coronavirus (COVID-19) pandemic. During the pandemic, there was a significant concentration of patients and challenging times in the health systems of all countries [4]. Global spread of the pandemic disrupted normal activities for millions of people worldwide [5]. According to the World Health Organisation, pneumonia claims approximately 3 million lives annually worldwide [6]. Additionally, pneumonia is responsible for around 700,000 child deaths each year, affecting 7% of the world's population [7].

The proliferation of chest X-rays has underscored the need to evaluate, design and develop a computer-aided diagnostic system for quick and reliable pneumonia diagnosis [1]. Relying solely on the visual examination of chest X-rays as a means of diagnosing pneumonia may lead to subjective findings and ultimately incorrect diagnoses [8]. Pramanik et al [9] proposed an alternative method for diagnosing pneumonia, utilising the particle swarm optimisation algorithm for feature selection on feature maps before classifying the extracted features using the k-nearest neighbors algorithm. This model displayed superior performance compared to both the pneumonia data set and various University of California Irvine data sets. Hemalatha [10] presented an optimised model based on Random Forest algorithm to deploy a pneumonia detection system. The introduced model was applied to IoT edge devices through cloud platforms and demonstrated efficiency in detecting pneumonia on the chest X-ray data set as well as the CT COVID19 data set. Toro et al. [11] conducted pneumonia detection from paediatric images using textural features. The authors achieved 83.3% accuracy with radiomics, 89.9% accuracy with fractal dimension and 91.3% accuracy with super pixel-based histogram using texture feature extraction techniques, which were then used to classify paediatric images using machine learning algorithms. In their study Fernandes et al. [12] employed Bayesian estimation for deep learning hyper-parameter optimisation and attained 96.4% accuracy without pre-processing or segmentation.

Mahmut et al. [13] efficiently extracted features using depth-wise convolution at varying dilation scales. The feature extraction was based on fine-tuning the feature extractor. Gradient-based localisation was used to detect anomalies in the images. Dey et al. [14] introduced a deep learning model that combined three different extraction techniques in the visual geometry group19 (VGG19) model [15]. According to the findings, the random forest model based on VGG19

achieved a success rate of 97.94%. In a study by Szepesi and Szilagyi [16] a precision of 97.2% was achieved by applying a dropout technique to a convolutional neural network (CNN). Moreover, the generative adversarial network method [17] was used for data augmentation on the samples in the data set. Ayan [18] performed pneumonia classification with Xception [19]. The research implemented transfer learning and fine-tuning on the Xception network for better performance. Instead of fully connected layers, classification was performed using different machine learning models. The results showed an accuracy rate of 89.74% using the Xception model. Gülgün and Erol [20] carried out pneumonia classification using three different CNN approaches. In this research data augmentation and transfer learning models were applied in conjunction with CNN. The models were subsequently assessed based on accuracy and loss. Based on the results, it was found that the application of data augmentation improved the accuracy of the CNN model, which outperformed the other models with an impressive accuracy of 93.4%.

Current methods for detecting pneumonia in chest X-ray images have persistent limitations and gaps, necessitating the investigation of more complex models. Challenges include inaccurate lung segmentation and the potential for false positive or negative results in pneumonia detection. Some models lack the capacity to capture the complex features associated with pneumonia, which is vital for accurate detection of subtle patterns and variations in the disease. Models trained on limited data sets pose a problem in terms of generalisation, especially in scenarios where there are differences in image quality and disease presentation. Moreover, some deep learning models are computationally intensive and have limited applicability in resource-constrained environments.

In this study we examined the categorisation of chest X-ray images into healthy and pneumonia categories using an advanced model designed in three stages. Firstly, X-ray images underwent histogram equalisation. Next, lung segmentation pre-processing was conducted in the second stage (image segmentation) utilising mask region-based CNN (mask R-CNN) model. Pneumonia detection was carried out in the third stage (classification) using pre-trained deep learning models, namely alex network (AlexNet), residual netwok18 (ResNet18) and visual geometry group16 (VGG16), on the processed images. The application of X-Ray image pre-processing to increase success, along with the fact that image segmentation and classification processes were performed with a 3-stage deep learning model, distinguishes this study from others in the literature.

METHODS

An open-source data set was obtained from the Kaggle platform [21]. The data set includes 5840 samples of chest X-ray images from children aged 1-5 years old and comprises 1575 healthy and 4265 pneumonia-infected chest X-ray images. The images in the data set belong to paediatric patients. Two sample X-ray images from the data set, one of a healthy patient and the other of a pneumonia-infected patient, are shown in Figure 1. The data set was classified into two classes using the pre-trained deep learning model.

The numbers of data used for training and testing are given in Table 1. The reason for selecting 234 healthy and 390 pneumonia images for testing is that the data on the Kaggle platform is divided in this manner. Previous studies in the literature have also made a similar distinction. For a fair comparison, the division in this study follows the same pattern.

The flow chart of the proposed model is shown in Figure 2. It consists of three stages. In the first stage histogram equalisation, an image processing method, was implemented to enhance the quality of chest X-Ray images. In the second stage the mask R-CNN (first-level deep learning)

Maejo Int. J. Sci. Technol. **2024**, *18*(01), 75-87

method segmented the rib cage of images precisely. In the last stage pneumonia was detected in segmented images using AlexNet, ResNet18 and VGG16 models (second-level deep learning). The success results of the models were compared using performance metrics.

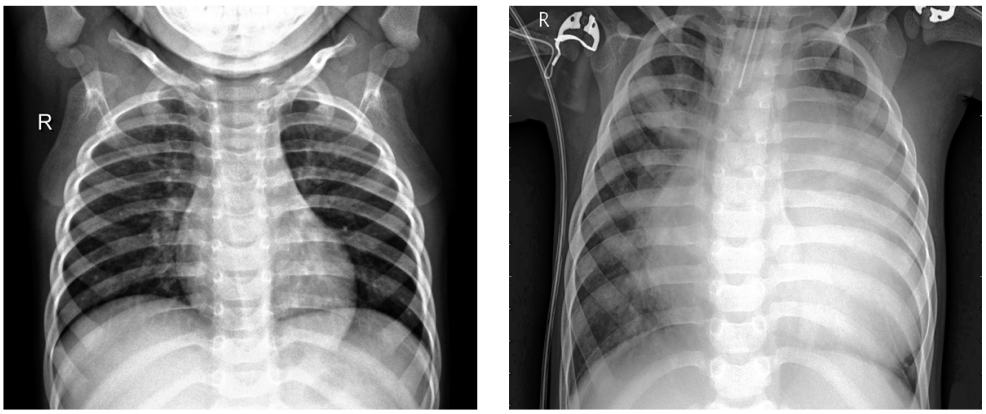

(a) (b)

Figure 1. Sample images of the data set: a) healthy image, b) pneumonia-infected image

Table 1. Number of data used for training and testing

	Healthy	Pneumonia
Training	1341	3875
Testing	234	390

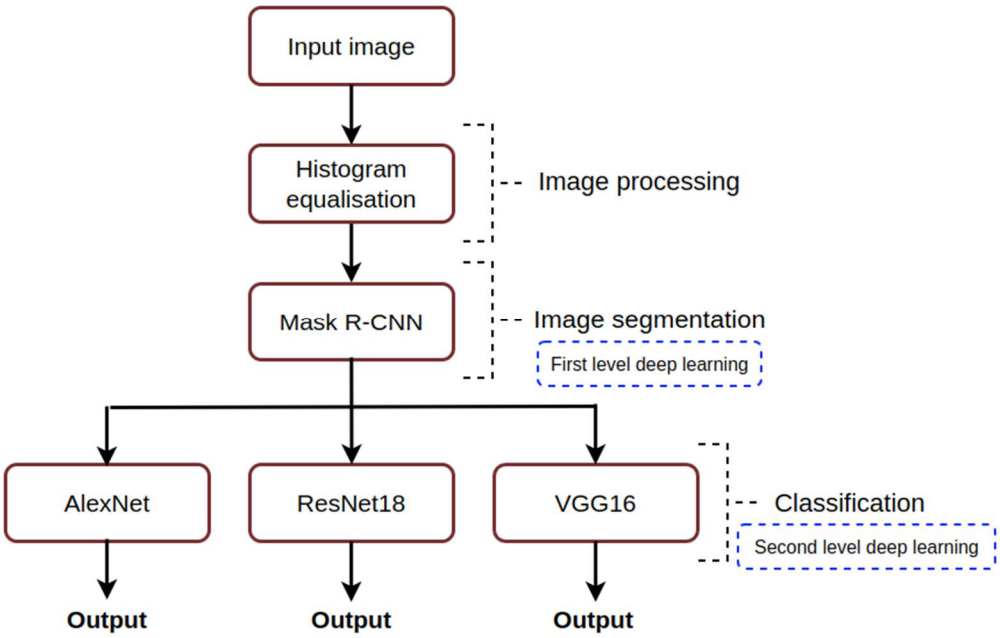

Figure 2. Flow chart of proposed model.

Histogram Equalisation

The process of determining the pixel histogram of an image gives information about the image quality. When pixel intensities are not evenly distributed in the histogram, there may be distortions in the contrast of the image. By increasing the contrast of the image through the

Maejo Int. J. Sci. Technol. **2024**, *18*(01), 75-87

histogram equalisation method, improvements can be made [22]. In this case more successful detection is achieved on the image. The probability distribution of pixel intensities is calculated using the following equation:

$$P(i) = \frac{n_i}{total}, i = 0,1, \dots, L-1 ,$$

where i stands for the grey pixel intensity, n_i for the quantity of grey pixels with that intensity, $total$ for the overall pixel count and $L-1$ represents the maximum grey pixel intensity. $P(i)$, the probability distribution used to perform contrast enhancement, is calculated using the following equation:

$$s_k = T(k) = (L-1)\sum_{i=0}^{k} P(i) ,$$

where s_k is the mapped image. The mapping function $T(k)$ operates on the grey pixel intensity i from the input image to produce the $P(i)$ image via the mapping function. Histogram equalisation applied to healthy and pneumonia X-ray images are shown in Figure 3.

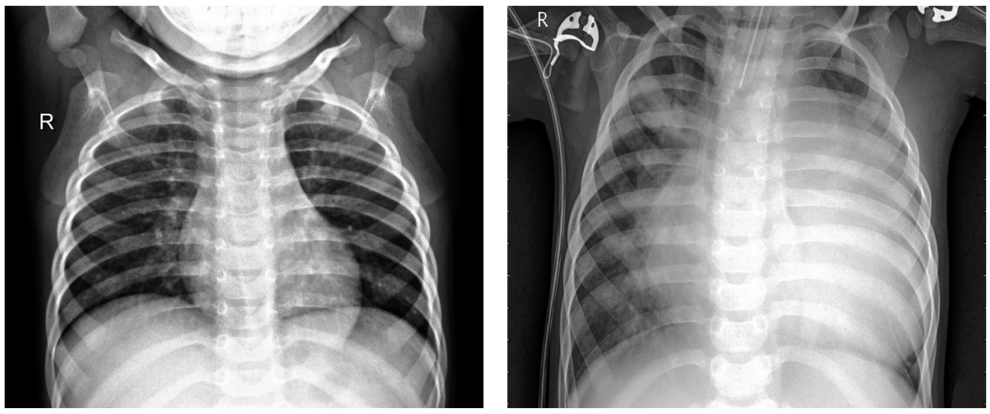

(a) (b)

Figure 3. Histogram equalisation applied to images: a) healthy image, b) pneumonia-infected image

When applying histogram equalisation in medical imaging, it is essential to consider certain limitations. While histogram equalisation is effective in enhancing contrast, it may overlook the semantic relationship of pixel intensities, leading to the potential loss of crucial diagnostic information. Additionally, its sensitivity to outliers and the possible increase in noise can jeopardise the accuracy of medical images, which often contain delicate structures and abnormalities.

Mask R-CNN

Mask R-CNN [23] uses a feature extractor to perform a region proposal network operation on feature maps [24]. This operation performs classification on anchor boxes to determine if an object is present and performs regression on the boxes to refine them [25]. The anchor boxes are pre-defined bounding boxes of different aspect ratios and scales used to cover various sizes and shapes of objects in the image.

For feature extraction in the mask R-CNN architecture, the ResNet101 backbone was employed. ResNet is known for its deep structure, addressing the vanishing gradient problem by introducing residual connections. ResNet101 consists of a series of building blocks called residual blocks, each of which contains multiple convolutional layers and enables the network to learn the residual functions through shortcut connections. This facilitates the training of very deep neural

Maejo Int. J. Sci. Technol. **2024**, *18*(01), 75-87

networks by mitigating the degradation problem, where adding more layers can result in worse performance. In this study mask R-CNN was used after histogram equalisation for determining the chest area. Sample images of healthy and pneumonia-infected cases obtained from the application of mask R-CNN method are shown in Figure 4.

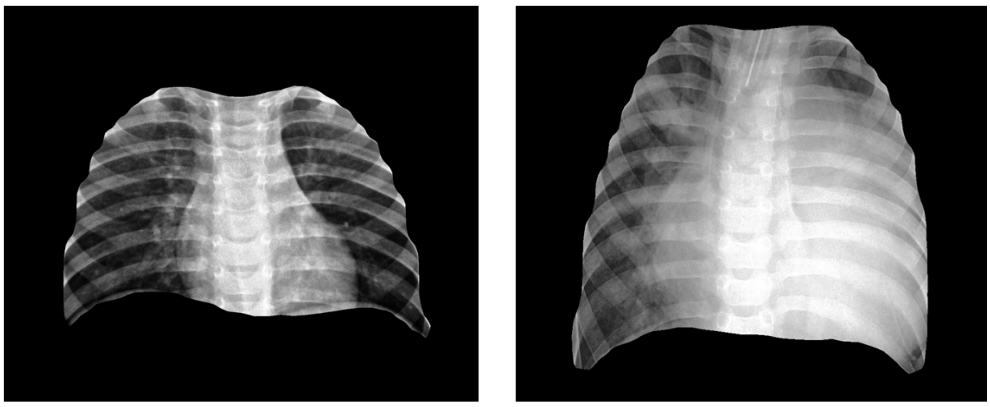

(a) (b)

Figure 4. Healthy image (a) and pneumonia-infected image (b) obtained from mask R-CNN method

Deep Learning Methods

Pre-trained models, a subset of deep learning methods, are becoming widely available [5]. In this study we tested and compared the performance of AlexNet, ResNet18 and VGG16, which are pre-trained deep learning methods.

AlexNet

AlexNet, proposed by Krizhevsky et al. [26], is one of the commonly used pre-trained deep learning methods. The designed model consists of a total of 8 layers; five of them are convolutional layers and three are fully connected layers. The network comprises 60 million parameters [27]. Since there are 1.2 million images in the ImageNet data set, AlexNet is trained in parallel using 2 graphics processing units [28]. The commonly used methods for training the models are the tanh and sigmoid activations, calculated using the following equations:

$$f(x) = tanh(x)$$

where x is the input to the tanh function, and

$$f(x) = \frac{1}{1+e^{-x}}$$

where e is the base of natural logarithm and x is the input to sigmoid function.

The AlexNet model is trained using the rectified linear unit activation function because it is a faster linear activation [27]. The function is calculated using the following equation:

$$f(x) = ma\,x(0, x).$$

In this study the pre-trained weights from the ImageNet data set were used for transfer learning. The binary classification of healthy and pneumonia patients were performed using the AlexNet model. Since there are two classes, 2 neurons were used in the fully connected layer instead of 1000 in the last layer and the softmax activation function was applied.

Maejo Int. J. Sci. Technol. **2024**, *18*(01), 75-87

ResNet18

ResNet18 [28] consists of 17 convolutional layers and 1 dense layer. The most important feature of ResNet18 is its inclusion of residual blocks. As the layers of the convolutional neural network model increase, the problem of vanishing gradients arises [29]. In residual blocks identity mapping allows the input to be transferred to the output convolution, solving the problem of vanishing gradients. A residual block is calculated using the following equation:

$$H(x) = F(x) + X$$

where X is the output of the previous layer, $H(x)$ is the final feature map and $F(x)$ is the residual function.

VGG16

Simonyan and Zisserman [30] proposed VGG models. VGG16 model consists of a total of 21 layers: 13 convolutional, 5 pooling and 3 dense layers. Sixteen of these layers are weighted [31]. VGG16 is widely used for feature extraction in the detection of small objects. This model has a small core of size 3×3 and optimal layers [32]. In this study transfer learning was performed using previously trained weights from the ImageNet data set and fully connected layers with the rectified linear unit activation function were utilised.

In this study AlexNet, ResNet18 and VGG16 were trained using the python torch framework on Google Colab. The training models were tested using 624 test images. The hyper-parameters of the training models are given in Table 2.

Table 2. Hyper-parameters of training models

Hardware(Graphics processing unit)	Tesla T4 (Compute unified device architecture)
Epoch:	50
Batch Size:	128
Workers:	4
Loss function:	Cross entropy
Optimiser:	Adam
Learning rate:	0.00001

Throughout the study the models underwent training for 50 epochs. Cross entropy loss function was employed, along with the adam optimiser and a learning rate of 0.00001. Training was executed using a batch size of 128 and was distributed among 4 workers. Models were tested using the weights obtained from the epoch where the best validation accuracy was achieved during the 50 epochs.

RESULTS AND DISCUSSION

Performance Comparison of AlexNet, ResNet18 and VGG16

In the study three models were compared using performance metrics. Performance results of the models are shown in Table 3. According to the table, the highest accuracy rate of 0.983 was achieved using ResNet18, indicating that healthy and pneumonia images are classified with the highest success by ResNet18. The VGG16 model performed the best based on the precision metric, with a precision rate of 0.992. Precision is a metric that depends on the false positive value in the confusion matrix. ResNet18 demonstrated the best performance in terms of the recall metric with a

Maejo Int. J. Sci. Technol. **2024**, *18*(01), 75-87

rate of 0.994. Recall is a metric that decreases as the number of false negatives in the confusion matrix increases.

Table 3. Performance results of the models

	Accuracy	Precision	Recall	F1-Score	AUC Score
AlexNet	0.972	0.969	0.987	0.978	0.972
ResNet18	0.983	0.979	0.994	0.987	0.969
VGG16	0.982	0.992	0.979	0.985	0.987

According to the results of this study, the best performance in terms of the F1-score is achieved using ResNet18, with a rate of 0.987. The fact that ResNet18 achieved the highest F1-score indicates that it is the model that provides the best trade-off between recall and precision metrics. The area-under-curve (AUC) score values for AlexNet, ResNet18 and VGG16 are 0.972, 0.969 and 0.987 respectively. The best performance in terms of AUC-score is achieved using VGG16 with a ratio of 0.987. The AUC-score is a metric that can be used to compare the overall performance of the models. Therefore, considering the AUC-score, VGG16 shows superior performance in classifying healthy and pneumonic images compared to the other models.

Training and validation accuracy graphs of AlexNet, ResNet18 and VGG16 are shown in Figure 5. The graph indicates that the peak training accuracy of 1.0 is reached at certain epoch values. Receiver operating characteristic curves of the models used in the study are shown in Figure 6. The AUC-score metric can be calculated from the curves. It is observed that the VGG16 model is more successful than the other models in the figure.

Maejo Int. J. Sci. Technol. **2024**, *18*(01), 75-87

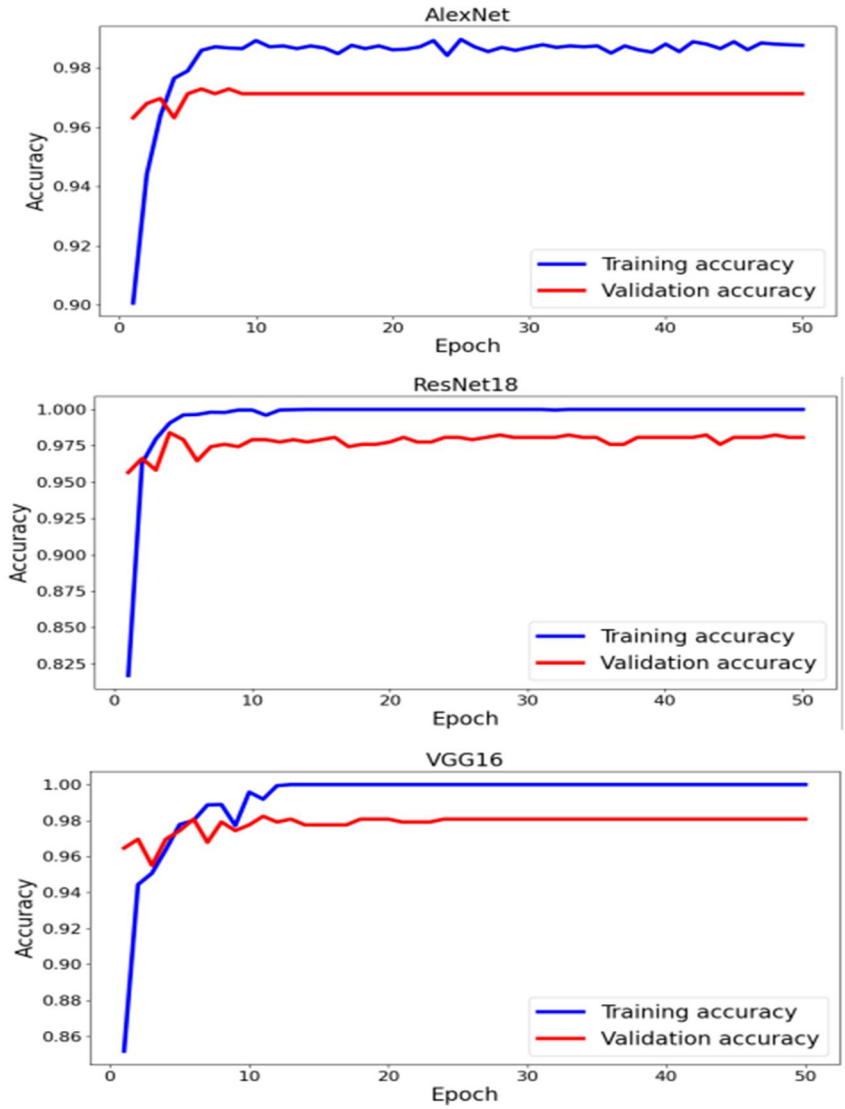

Figure 5. Comparison of the training and validation accuracy of AlexNex, ResNet18 and VGG16

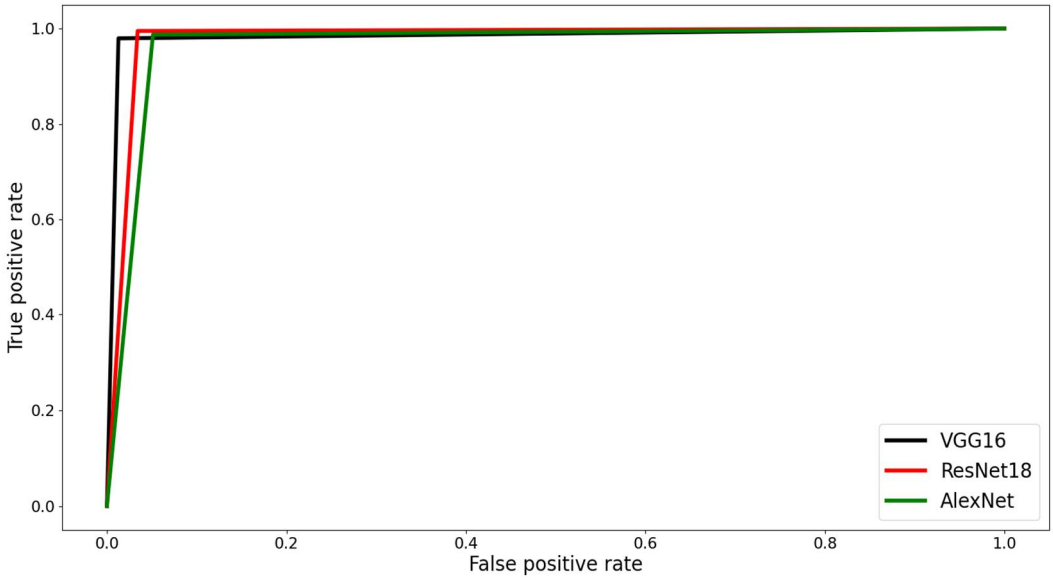

Figure 6. Comparison of receiver operating characteristic curves of AlexNet, ResNet18 and VGG16 models

Maejo Int. J. Sci. Technol. **2024**, *18*(01), 75-87

Comparison of AlexNet, ResNet18 and VGG16 with Studies in Literature

A comparison of the employed models with previous studies from the literature is shown in Table 4. Pramanik et al. [9] proposed the ResNet50+PSO model, which demonstrated superior performance with the highest accuracy rate. Among all the studies, this model achieved an accuracy rate of 0.9841, making it the most successful in classifying the samples.

Table 4. Comparison of proposed models with studies in literature

Reference	Method	Accuracy	Precision	Recall	F1-Score	AUC-Score
Pramanik et al.[9]	ResNet50+PSO	0.9841	0.9880	0.9902	0.9902	-
Dey et al.[14]	VGG19-DT	0.9745	0.9454	-	0.9537	-
Mahmud et al.[13]	CovXNet	0.981	0.98	0.985	0.983	0.994
Rajaraman et al.[33]	VGG16	0.962	0.977	0.962	0.970	0.993
Liang et al.[34]	CNN	0.905	0.891	0.967	0.927	0.953
Fernandes et al.[12]	CNN	0.964	0.964	0.979	0.972	
Proposed models	AlexNet	0.9727	0.9697	0.9871	0.9783	0.9678
	ResNet18	0.9839	0.9797	0.9948	0.9872	0.9803
	VGG16	0.9823	0.9922	0.9794	0.9858	0.9833

ResNet18 employed in this work has an accuracy value of 0.983, which is extremely similar to the accuracy value of the model presented by Pramanik et al. [9]. The best precision performance, with a value of 0.992, was obtained using the VGG16 model we proposed. The VGG16 model used in this study has the least number of misclassifications of healthy images as pneumonia.

In terms of recall, the ResNet18 model used in this study achieves superior performance compared to other studies with a rate of 0.994. This indicates that the ResNet18 model is one that detects pneumonia images with the least amount of error. The best performance in terms of F1-score, with a value of 0.990, was obtained using the ResNet50+PSO model proposed by Pramanik et al. [9]. The model provides the best trade-off between recall and precision. The ResNet18 model proposed in this study also performs well with an F1-Score of 0.987.

The CovXNet model proposed by Mahmud et al. [13] achieves the highest success in terms of AUC-score, with a rate of 0.994, compared to other studies. Dey et al. [14] proposed the VGG19-DT method and achieved an accuracy of 0.974, precision of 0.945 and an F1-Score of 0.953 success rate. The accuracy value of VGG19-DT is higher than that of the AlexNet used in this study. However, it is lower than those of the ResNet18 and VGG16 models used in this study. The AUC-score of VGG16 proposed by Rajaraman et al. [33] is 0.993. This is higher than that achieved by the VGG16 used in this study. The VGG16 model utilised in this study showcases improved performance when compared to that proposed by Rajaraman et al. [33]. The former achieves higher accuracy, meaning more correct predictions as well as better precision, which indicates its ability to minimise false positives.

Furthermore, the VGG16 model in this study demonstrates superior recall, signifying its capability to reduce false negatives, leading to an overall higher F1-score that indicates a better balance between precision and recall. The CNN proposed by Liang and Zheng [34] has a recall rate of 0.967. Furthermore, the CNN proposed by Fernandes et al. [12] achieved a recall rate of 0.979. This model's recall rate is higher than that of the CNN proposed by Liang and Zheng [34].

In addition, the use of intelligent disease diagnostic decision systems, both inside and outside of hospital environments (located in different locations online), has become widespread

[35]. In this study we observe the successful utilisation of deep learning models in intelligent diagnostic systems with high accuracy.

CONCLUSIONS

The study achieves high performance success in detecting pneumonia through the use of pre-trained deep learning models. The proposed model is able to enhance the accuracy and efficiency of diagnosing pneumonia, ultimately leading to saving lives. In future research our objective is to utilise this three-stage advanced deep learning model for detecting other illnesses in medical images.

However, we encountered some limitations during the research process. A notable constraint is associated with the data set used, encompassing considerations of diversity. Problems in obtaining labelled data for training and the difficulty in obtaining a truly representative data set may affect the generalisability of the proposed model. Additionally, the hyper-parameter tuning process introduced challenges that could affect the reproducibility and robustness of the findings. These limitations underscore the need for future research to address these challenges and emphasise the necessity for overcoming these limitations in future studies.

ACKNOWLEDGEMENTS

The authors wish to thank the referees for useful comments and suggestions.

REFERENCES

1 S. Sangeetha, S. Suruthika, S. Keerthika, S. Vinitha and M. Sugunadevi, "Diagnosis of pneumonia using image recognition techniques", Proceedings of 7th International Conference on Intelligent Computing and Control Systems , **2023**, Madurai, India, pp.1332-1337.

2 N. P. Tembhare, P. U. Tembhare and C. U. Chauhan, "Chest X-ray analysis using deep learning", *Int. J. Res. Appl. Sci. Eng. Technol.*, **2023**, *11,* 1441-1447.

3 A. Gupta, M. Padsala and P. Saikia, "Detection of pneumonia from chest X-ray images using transfer learning on deep CNN", Proceedings of 4th International Conference for Emerging Technology , **2023**, Belgaum, India, pp.1-6.

4 K. Rajpurohit and T. Sandhan, "Improved pneumonia diagnosis of radiological images using hybrid loss with conventional CNN", Proceedings of International Conference on Microwave, Optical and Communication Engineering, **2023**, Bhubaneswar, India.

5 A. N. Salama, M. A. Mohamed, H. M. Amer and M. M. Ata, "An efficient quantification of COVID-19 in chest CT images with improved semantic segmentation using U-Net deep structure*", Int. J. Imag. Syst. Technol*, **2023**, *33*, 1882-1901.

6 World Health Organization, "WHO coronavirus (COVID-19) dashboard", **2023**, https://covid19.who.int/ (Accessed: April 2023).

7 M. F. Hashmi, S. Katiyar, A. G. Keskar, N. D. Bokde and Z. W. Geem, "An efficient pneumonia detection in chest Xray images using deep transfer learning", *Diagnost.*, **2020**, *10*, Art.no.417.

8 R. Chiwariro and J. B. Wosowei, "Comparative analysis of deep learning convolutional neural networks based on transfer learning for pneumonia detection", *Int. J. Res. Appl. Sci. Eng. Technol.*, **2023**, *11*, 1161-1170.

9 R. Pramanik, S. Sarkar and R. Sarkar, "An adaptive and altruistic PSO-based deep feature selection method for pneumonia detection from chest X-rays", *Appl. Soft Comput.*, **2022**, *128*, Art.no.109464.
10 M. Hemalatha, "A hybrid random forest deep learning classifier empowered edge cloud architecture for covid-19 and pneumonia detection", *Expert Syst. Appl.*, **2022**, *210*, Art.no.118227.
11 C. Ortiz-Toro, A. García-Pedrero, M. Lillo-Saavedra and C. Gonzalo-Martín, "Automatic detection of pneumonia in chest X-ray images using textural features", *Comput. Biol. Med.,* **2022**, *145*, Art.no.105466.
12 V. Fernandes, G. B. Junior, A. C. de Paiva, A. C. Silva and M. Gattass, "Bayesian convolutional neural network estimation for pediatric pneumonia detection and diagnosis", *Comput. Meth. Program Biomed.*, **2021**, *208*, Art.no.106259.
13 T. Mahmud, M. A. Rahman and S. A. Fattah, "CovXNet: A multi-dilation convolutional neural network for automatic Covid-19 and other pneumonia detection from chest X-ray images with transferable multi-receptive feature optimization", *Comput. Biol. Med.*, **2020**, *122*, Art.no.103869.
14 N. Dey, Y. Zhang, V. Rajinikanth, R. Pugalenthi and N. S. M. Raja, "Customized VGG19 architecture for pneumonia detection in chest X-rays", *Pattern Recogn. Lett.*, **2021**, *143*, 67-74.
15 T.-H., Nguyen, T.-N., Nguyen, B.-V. Ngo, "A VGG-19 model with transfer learning and image segmentation for classification of tomato leaf disease", *AgriEng.*, **2022**, *4*, 871-887.
16 P. Szepesi and L. Szilagyi, "Detection of pneumonia using convolutional neural networks and deep learning", *Biocybern. Biomed. Eng.*, **2022**, *42*, 1012-1022.
17 I. J. Goodfellow, J. Ponget-Abadie, M. Mirza, B. Xu, D. Warde-Farley, S. Ozair, A. Courville and Y. Bengio, "Generative adversarial networks", **2014**, https://arxiv.org/abs/1406.2661 (Accessed: June 2023).
18 E. Ayan, "Using a convolutional neural network as feature extractor for different machine learning classifiers to diagnose pneumonia", *Sakarya Univ. J. Comput. Inform. Sci.*, **2022**, *5*, 48-61.
19 F. Chollet, "Xception: Deep learning with depthwise separable convolutions", Proceedings of IEEE Conference on Computer Vision and Pattern Recognition, **2017**, Honolulu, USA, pp. 1800-1807.
20 O. D. Gülgün and H. Erol, "Classification performance comparisons of deep learning models in pneumonia diagnosis using chest X-ray images", *Turk. J. Eng.*, **2020**, *4*, 129-141.
21 D. Kermany, K. Zhang and M. Goldbaum, "Labeled Optical Coherence Tomography (OCT) and Chest X-ray Images for Classification" (Mendeley Data, Version 2), University of California San Diego, San Diego, **2018**.
22 F. Bulut, "A new histogram equalization method with modified discrete Haar Wave Transform", *J. Eng. Sci. Design*, **2022**, *10*, 188-200.
23 K. He, G. Gkioxari, P. Dollar and R. Girshick, "Mask R-CNN", Proceedings of IEEE International Conference on Computer Vision, **2017**, Venice, Italy, pp.2980-2988.
24 D. R. Loh, W. X. Yong, J. Yapeter, K. Subburaj and R. Chandramohandas, "A deep learning approach to the screening of malaria infection: Automated and rapid cell counting, object

detection and instance segmentation using Mask R-CNN", *Comput. Med. Imag. Graph*, **2021**, *88*, Art.no.101845.

25 S. Ren, K. He, R. Girshick and J. Sun, "Faster R-CNN: Towards real-time object detection with region proposal networks", *IEEE Trans. Pattern Anal. Mach. Intel.*, **2017**, *39*, 1137-1149.

26 A. Krizhevsky, I. Sutskever and G. E. Hinton, "ImageNet classification with deep convolutional neural networks", *Commun. ACM*, **2017**, *60*, 84-90.

27 B. He, "Deep learning algorithm for facial expression classification", Proceedings of 3rd International Conference on Computer Vision, Image and Deep Learning and International Conference on Computer Engineering and Applications, **2022**, Changchun, China, pp.386-391.

28 K. He, X. Zhang, S. Ren and J. Sun, "Deep residual learning for image recognition", Proceedings of IEEE Conference on Computer Vision and Pattern Recognition, **2016**, Las Vegas, USA, pp.770-778.

29 T. Tian, L. Wang, M. Luo, Y. Sun and X. Liu, "ResNet-50 based technique for EEG image characterization due to varying environmental stimuli", *Comput. Meth. Programs Biomed.*, **2022**, *225*, Art.no.107092.

30 K. Simonyan and A. Zisserman, "Very deep convolutional networks for large-scale image recognition", **2014**, https://arxiv.org/abs/1409.1556 (Accessed: September 2023).

31 O. Sevli, "Performance comparison of different pre-trained deep learning models in classifying brain MRI images", *Acta Infologica*, **2021**, *5*, 141-154.

32 Y. Zamanidoost, N. Alami-Chentoufi, T. Ould-Bachir and S. Martel, "Efficient region proposal extraction of small lung nodules using enhanced VGG16 network model", Proceedings of IEEE 36th International Symposium on Computer-Based Medical Systems, **2023**, L'Aquila, Italy, pp.483-488.

33 S. Rajaraman, S. Candemir, I. Kim, G. R. Thoma and S. K. Antani, "Visualization and interpretation of convolutional neural network predictions in detecting pneumonia in pediatric chest radiographs", *Appl. Sci.*, **2018**, *8*, Art.no.1715.

34 G. Liang and L. Zheng, "A transfer learning method with deep residual network for pediatric pneumonia diagnosis", *Comput. Meth. Programs Biomed.*, **2020**, *187*, Art.no.104964.

35 N. A. Ghani, U. Iqbal, S. Hamid, Z. Jaafar, F. D. Yusop and M. Ahmad, "Methodical evaluation of healthcare intelligence for human life disease detection", *Malaysian J. Comput. Sci.*, **2023**, *36*, 208-222.